

AD-A041 858

ARMY ELECTRONICS COMMAND FORT MONMOUTH N J
AUTOMATION OF LONG-PATH ABSORPTION CELL MEASUREMENTS. (U)
JUN 77 W R WATKINS, R G DIXON
ECOM-5821

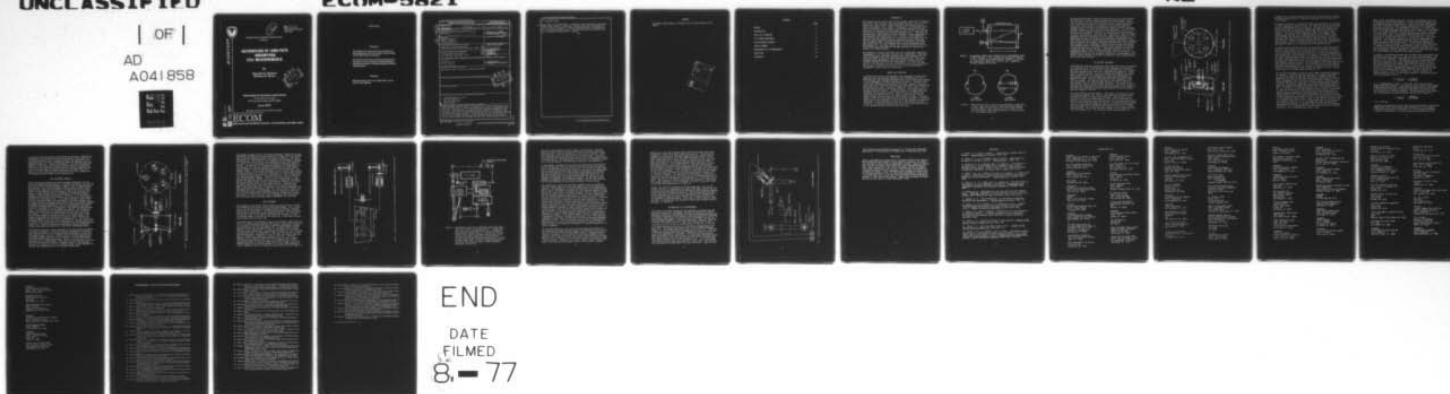
F/G 9/3

UNCLASSIFIED

| OF |

AD
A041858

NL





12
B.S.

AD

Reports Control Symbol
OSD-1366

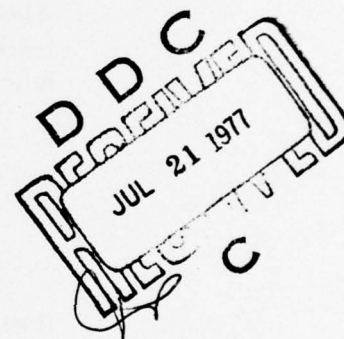
RESEARCH AND DEVELOPMENT TECHNICAL REPORT
ECOM-5821

AD A 041858

AUTOMATION OF LONG-PATH ABSORPTION CELL MEASUREMENTS

By

Wendell R. Watkins
Richard G. Dixon



Atmospheric Sciences Laboratory

US Army Electronics Command
White Sands Missile Range, New Mexico 88002

June 1977

Approved for public release; distribution unlimited.

AD No. _____
DDC FILE COPY

.....
ECOM

UNITED STATES ARMY ELECTRONICS COMMAND - FORT MONMOUTH, NEW JERSEY 07703

NOTICES

Disclaimers

The findings in this report are not to be construed as an official Department of the Army position, unless so designated by other authorized documents.

The citation of trade names and names of manufacturers in this report is not to be construed as official Government indorsement or approval of commercial products or services referenced herein.

Disposition

Destroy this report when it is no longer needed. Do not return it to the originator.

REPORT DOCUMENTATION PAGE		READ INSTRUCTIONS BEFORE COMPLETING FORM
1. REPORT NUMBER ECOM-5821	2. GOVT ACCESSION NO.	3. RECIPIENT'S CATALOG NUMBER Research and development
4. TITLE (and Subtitle) AUTOMATION OF LONG-PATH ABSORPTION CELL MEASUREMENTS.	5. TYPE OF REPORT & PERIOD COVERED R&D Technical Report	
7. AUTHOR(s) Wendell R. Watkins Richard G. Dixon	6. PERFORMING ORG. REPORT NUMBER	
9. PERFORMING ORGANIZATION NAME AND ADDRESS Atmospheric Sciences Laboratory White Sands Missile Range, New Mexico 88002	8. CONTRACT OR GRANT NUMBER(s)	
11. CONTROLLING OFFICE NAME AND ADDRESS US Army Electronics Command Fort Monmouth, New Jersey 07703	10. PROGRAM ELEMENT, PROJECT, TASK AREA & WORK UNIT NUMBERS 1L161102B53A-S329	
14. MONITORING AGENCY NAME & ADDRESS (if different from Controlling Office) 21p.	12. REPORT DATE June 1977	
	13. NUMBER OF PAGES 26	
	15. SECURITY CLASS. (of this report) UNCLASSIFIED	
16. DISTRIBUTION STATEMENT (of this Report) Approved for public release; distribution unlimited.		
17. DISTRIBUTION STATEMENT (of the abstract entered in Block 20, if different from Report)		
18. SUPPLEMENTARY NOTES		
19. KEY WORDS (Continue on reverse side if necessary and identify by block number) Long-path absorption cells Path differencing Precision gear drive Remote control		
20. ABSTRACT (Continue on reverse side if necessary and identify by block number) Recent advances have been made in the operation of long-path absorption cells which make them easier to align and improve the accuracy of measurements made with them. Only one person is required now for routine measurements of low absorption coefficients of atmospheric absorbers that have significant impact on Army electro-optical systems. Unique gear designs for the adjustment of the cell mirrors are described which utilize low-torque linear drives and make possible rapid changes in pathlength and precision repositioning of the cell		

DDC
JUL 21 1977
C

20. Abstract (cont)

→ output beam at long pathlengths. Automation of cell operation by the use of remote selsyn controls is described. Several techniques are discussed for precision optical alignment of long-path absorption cells, including the use of infrared radiation sources. The system accuracy which results from these refinements in operation is included. ↑

PREFACE

The authors thank James B. Gillespie for his timely review of this report.

ACCESSION FOR	
NTIS	White Section <input checked="" type="checkbox"/>
DOC	Buff Section <input type="checkbox"/>
UNANNOUNCED	
JUSTIFICATION	
BY	
DISTRIBUTION/AVAILABILITY CODES	
Dist.	AVAIL. AND/OR SPECIAL
A	

CONTENTS

	Page
PREFACE	1
INTRODUCTION	3
BASIC CELL OPERATION	3
CELL MIRROR ADJUSTMENT	5
NEW ADJUSTMENT CONTROLS	9
LASER ALIGNMENT	11
REPRODUCIBILITY OF MEASUREMENTS	15
CONCLUSION	17
REFERENCES	18

INTRODUCTION

Army applications of electro-optical (EO) systems, especially high-energy lasers (HEL) and long-range laser and broadband systems, such as laser designators, range finders, image intensifier and infrared imagers, remote wind sensors, etc., require a knowledge of low absorption coefficients of atmospheric constituents. An absolute measure of the weak absorptions (a few percent per kilometer or less) is difficult to obtain even with very sophisticated long-path absorption cells. Sometimes the concentration of weak absorbers can be increased to make measurement of the absorption coefficients easier [1]. However, self-broadening of gases [2] and even condensation, as in the case of water vapor [3], can severely limit how much the absorber concentration can be increased. Once an absolute measure of weak absorbers is obtained by using long-path absorption cells, spectrophones can be used to complement these measurements [4]. The basic problem then is obtaining the initial very accurate absolute measurement of the weak absorbers of interest and doing so in a timely fashion.

The Atmospheric Sciences Laboratory (ASL) has already made substantial improvements in its long-path absorption cell capabilities. Data acquisition and analysis have been automated [5,6], and techniques for reducing long-term system drift have been developed [7,8]. This report discusses system developments which improve the accuracy and fully automate long-path absorption cell measurements. In fact, only one person is now required to perform long-path absorption cell experiments. The savings in experimental man-hours as well as the improvement in measurement accuracy are quite significant.

BASIC CELL OPERATION

A detailed description of an absorption cell experiment is given elsewhere [9] as is the improved technique, path differencing [7], for obtaining data from long-path absorption cells by utilizing rapid changes in cell pathlength to minimize long-term drift error. The basic principles and procedures are described briefly here. Figure 1 gives the basic setup for a long-path absorption cell experiment using conventional White-type optics [10]. A source of radiation, in this case a laser, is divided into two portions by a beam splitter B. One portion goes to a reference detector system R. The other portion of the beam enters the absorption cell through a window W; makes multiple reflections from spherically concave mirrors M_1 , M_2 , and M_3 ; exits the cell through another window; and then goes to a sample detector system S. The pathlength in the cell can be determined by counting the number of reflection spot images in the multipath on mirror M_2 as seen through an observation window OW. A short multipath (1-spot) and a long multipath (N-spot) (Figure 2) are obtained by adjusting only mirror M_3 once mirrors M_1 and M_2 are appropriately positioned as described later.

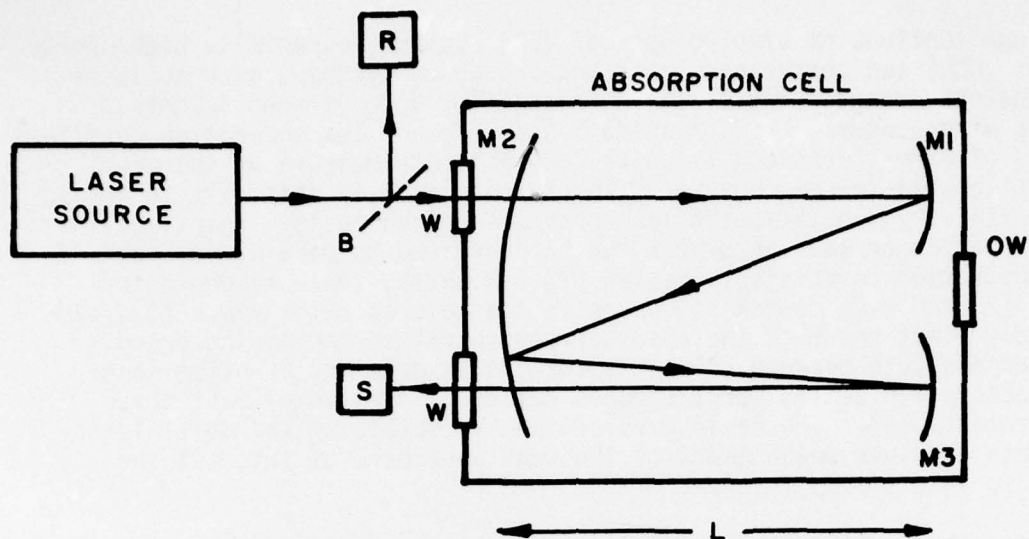


Figure 1. Conventional "White-type" absorption cell experimental setup: B, beam splitter; W, cell windows; OW, observation window; R and S, reference and sample detector systems; M_1 , M_2 , and M_3 , spherically concave cell mirrors; and L, separation distance between cell mirrors.

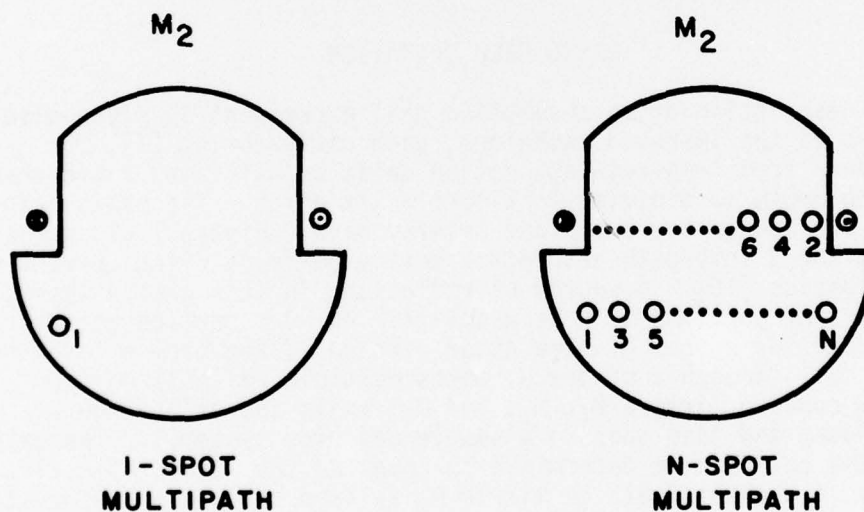


Figure 2. Views of mirror M_2 as seen from the observation window OW for a 1-spot (left) and an N-spot (right) multipath; numbered circles, images of laser source on mirror surface; circle with central dot, laser beam entering cell; and circle with "X," laser beam exiting cell.

Absorption coefficients of gases are measured by using a path differencing technique of rapidly taking reference and sample detector signal data for short l-spot and long N-spot multipaths. Basically, absolute cell transmittance values for the optical path difference between an N-spot and l-spot multipath are obtained by taking short-term time averaged ratios of relative transmittances (sample divided by reference detector signals) for the N-spot and l-spot multipaths. The cell transmittance values obtained contain mirror reflectance loss and gaseous absorption contributions. Two such cell transmittance values are needed to obtain the absorption coefficient for a specific gas--one for a cell atmosphere with the absorbing gas and one without the absorbing gas. To obtain good accuracy in low absorption coefficient measurements, long-term drift error which plagues long-path absorption cells must be reduced. Path differencing which nearly eliminates long-term drift error requires rapid changes in cell pathlength, including precision beam positioning. Exact repositioning of the beams formed on mirror surfaces is essential in reducing long-term system drift. Long-path absorption cell optical systems designed to obtain maximum output beam stability by use of compensating optics [11] do so at the expense of mirror reflection loss reproducibility because the systematic cancelation of beam wander by the optical system inherently precludes the checking of exact beam positioning on the mirror surfaces.

CELL MIRROR ADJUSTMENT

A description of how the conventional White-type cell mirrors are mounted in a long-path cell is required before their adjustment is discussed. The optics of the ASL 21-m stainless steel absorption cell will be used here and throughout this report as a representative example of a long-path cell optical system. The mirror holders and mechanism for attachment to the 21-m cell are adaptations of the mirror system used in a 2-m stainless steel cell purchased from Boller-Chivens (Contract No. DAAD07-71-C-0254). Figure 3 illustrates the basic components of the 21-m cell system. The mounting rings (one in each end of the cell), which support the cell mirror holders and mirrors, are secured to the cell wall by a set of pressure plates and bolts. Each mirror holder is attached to the mounting ring on two large threaded bolts and secured by pairs of nuts, which makes possible positioning of the mirror holders along the length of the cell.

The mirror holders are more complex. They consist of three parts which are connected together (the first to the second and the second to the third) by two sets of spring-loaded flexures. These flexures allow rotation of the mirror-holding portion of the mirror holder about the vertical and horizontal axes of the mounting ring by moving two pressure rods in or out along the length of the cell. The two-mirror-end pressure rods are linear motion feedthroughs which push against contact plates and are attached to the two-mirror end flange of the cell by a flanged vacuum bellows. This allows the mirror holders to be adjusted from outside the evacuable cell. The single-mirror-end pressure rods are

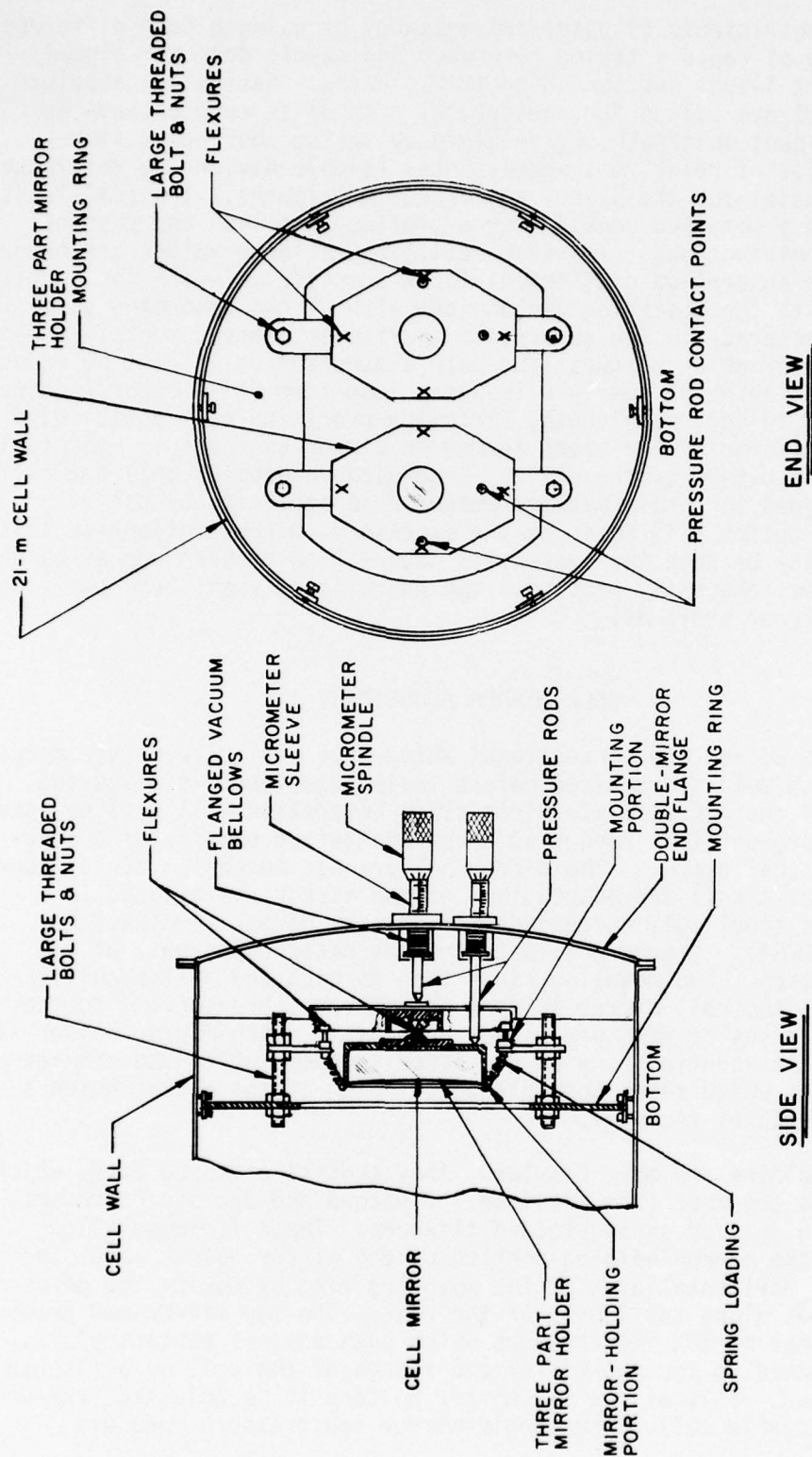


Figure 3. End and side views of mounting ring, three-piece mirror holders with spring loaded flexures, and double-mirror end cell flange with flanged vacuum bellows and pressure rods.

threaded into the mounting portion of the mirror holder and are initially positioned inside the cell. Additional adjustment of the single mirror is not needed.

The optical system for a conventional White-type absorption cell consists of three spherically concave mirrors, one at one end and two at the other end of an absorption cell as in Figure 1. The radii of curvature of all three mirrors and the separations between the single mirror and either of the two mirrors at the opposite end of the cell are all of equal length L . This forms a beam conserving system. The f-number of the entrance beam into the cell is adjusted, by a pair of concave mirrors placed between the laser and the beam splitter in Figure 1, to focus the beam in the plane of mirror M_2 and to irradiate a large portion of the mirror M_1 . Mirror M_1 focuses the beam onto mirror M_2 . The reflected beam diverges to fill a large portion of mirror M_3 and then refocuses in the plane of mirror M_2 as it passes out of the absorption cell.

The above optical configuration does not give the best beam conservation. Focusing on the surface of mirror M_2 can greatly accentuate the effects of mirror imperfections such as a speck of dust or small pit in terms of mirror reflection losses and reproducibility. To avoid such degradation, a collimated beam a few millimeters in diameter is introduced into the cell. Mirror M_1 focuses the beam midway along the length of the cell, and mirror M_2 sends a collimated beam to mirror M_3 which in turn focuses the beam midway along the length of the cell. The cell output beam (circle with "X") thus becomes a diverging beam of the same diameter as the input beam (circle with dot) upon leaving the cell. This configuration limits the maximum obtainable pathlength of the cell because the spots on mirror M_2 are not focused to a small diameter; but no beams are focused on mirror surfaces, which results in far better beam conservation [7].

The initial positioning of mirror M_2 with respect to mirrors M_1 and M_3 is important. To begin, the input beam has its f-number adjusted as in the first case above, so that the input beam is focused inside the absorption cell just off the input window upper right edge of mirror M_2 and in the plane of its reflecting surface as shown in Figure 2. The diverging beam from this focal point is then centered on the surface of mirror M_1 . Mirror M_1 is adjusted to focus the reflected beam directly below the output window upper left edge of mirror M_2 , again shown by spot 1 in Figure 2. If the beam does not focus on the surface of mirror M_2 , then the separation distance between mirrors M_1 and M_2 is not equal to their radii of curvature. Mirror M_1 must be repositioned and the above procedure repeated until the beam from mirror M_1 focuses at the surface of mirror M_2 . The diverging beam from the surface of mirror M_2 is then centered on the surface of mirror M_3 by adjusting mirror M_2 about its horizontal and vertical axes. Mirror M_3 may need to be moved closer to or farther from mirror M_2 if its return beam does not also focus at the surface of mirror M_2 . This adjustment maximizes the obtainable pathlength and minimizes the chance of beam clipping inside the absorption cell. This is true whether the input beam is focused in the plane of mirror M_2 or a collimated input beam is used.

After initial positioning of the cell mirrors, the absorption cell can be sealed and used for measurements. To obtain maximum pathlength, the collimated input beam is positioned as close to the upper right edge of mirror M_2 as possible without causing clipping and is also centered in the middle of mirror M_1 . The adjustment of mirror M_1 is critical for obtaining maximum pathlength and allowing rapid changes of the pathlength from 1- to N-spot multipaths with only mirror M_3 . The spot 1 in Figure 2 is positioned so that it is centered directly below the left edge of mirror M_2 and an equal distance below the horizontal optical axis of mirror M_2 as the exit spot with the "X" is above the axis. The latter adjustment is performed in conjunction with vertical adjustments of mirror M_3 . The 1-spot multipath output beam can be centered on the sample detector by adjusting mirror M_3 . If horizontal adjustment of the mirror M_3 does not produce a long N-spot multipath output beam which is centered vertically on the sample detector system, the spot 1 on mirror M_2 must be appropriately raised or lowered by adjusting mirror M_1 with corresponding vertical adjustment of mirror M_3 until both the 1-spot and N-spot outputs are centered on the sample detector.

In practice, the multipath outputs must be repositioned horizontally and vertically to within 1 mm for a 1-spot to 37-spot path difference. This path difference represents a pathlength of 1,512 m for the 21-m absorption cell (i.e., $2(N-1)L$). This puts restrictions on how precise the smallest adjustment of the linear feedthrough pressure rods must be. The contact points of the pressure rods and mirror holders are 114 mm from the corresponding axis of rotation. A small angular rotation of mirror M_3 will cause a corresponding angular offset of the output beam of twice the rotation angle for each reflection from mirror M_3 or $2[(\text{No. of spots} + 1)/2] = \text{No. of spots} + 1$. Hence, to obtain 1 mm repositioning error for a 37-spot output requires a linear motion error (x) of the pressure rods of

$$38 \left(\frac{x}{114 \text{ mm}} \right) = \left(\frac{1 \text{ mm}}{21,000 \text{ mm}} \right)$$

or $x = 0.000143 \text{ mm}$ or $0.143 \mu\text{m}$. In addition, to be able to rapidly change pathlengths between 1- and N-spot multipaths requires the movement of the output beam for the 1-spot multipath (makes only one reflection from mirror M_3) a distance of 279 mm in the plane of mirror M_2 to the spot 2 position in a 37-spot multipath. The corresponding linear motion (y) of the pressure rod controlling the vertical axis rotation is

$$2 \left(\frac{y}{114 \text{ mm}} \right) = \left(\frac{279 \text{ mm}}{21,000 \text{ mm}} \right)$$

or $y = 0.757 \text{ mm}$.

Initially, the pressure rods were adjusted by using bakeable linear motion feedthroughs Ultek (Perkin Elmer) Model 282-6200 with 1.57 thread/mm micrometer spindle drive and accuracy of 0.127 mm including backlash. To meet the requirement y of rapidly changing pathlength was trivial;

a little over one revolution of the spindle was necessary. Meeting the requirement of rapidly obtaining the repositioning of the output for a 37-spot multipath was nearly impossible because the magnitude of the repositioning error of the micrometer was about one thousand times that required to meet the x repositioning demands. Two major problems were inherent in the system, excluding the minor problem of gear backlash. First, the torque required to obtain the drive accuracy needed was too small for direct manual micrometer operation; and second, the drive controls for the system were at one end of the 21-m cell, whereas the cell output had to be viewed from the opposite end.

NEW ADJUSTMENT CONTROLS

Both of the above problems have been eliminated through use of a new drive gear design and remote selsyn (or synchronous) motors; and yet, the ability to rapidly change pathlengths between 1- and 37-spot multipaths was retained. First to be addressed is the problem of spindle torque. Several system components were added to the end of the cell to allow control of the pressure rods from outside a 20 cm thick heating shell which is around the entire cell for bakeout and temperature control purposes. These changes are depicted in Figure 4. A 1-1/4-cm thick aluminum base plate was offset from the cell's two-mirror end flange by several 2-1/2-cm diameter bolts. This plate was used to rigidly hold all gears required to make fine adjustments of the four pressure rods. The linear motion feedthroughs were used but without the spindle attached. An extension rod was threaded into the end of the pressure rod instead. A Starrett micrometer Model 262RL with 1.57 thread/mm was attached to the end of the extension rod and mounted to the outside of the aluminum plate. The operation of the micrometer was altered. The spindle was secured to the drive rod by tightening the end nut after the ratchet was removed. The allen bolt which screws into the guide slot in the drive rod was removed to allow the drive rod to rotate freely in the mounting sleeve when the spindle-drive rod unit (which includes the spindle attached to the drive rod) is threaded onto it. The result is a micrometer drive which, when the mounting sleeve is rotated, a nonrotating drive of the spindle-drive rod is obtained with only micrometer drive thread slop. Even this problem was eliminated by spring loading the pressure rod extension against the linear motion feedthrough sleeve.

The problem of the small torque required to fine position the micrometer drive was alleviated by a precision worm gear operated 25:1 reduction gear mounted directly to the aluminum plate and secured to the Starrett micrometer sleeve. Again, no rotation slop of the reduction gear was encountered because the whole drive mechanism is spring loaded against the linear motion feedthrough sleeve. There is a little slop in the worm gear, but no corresponding linear motion of the pressure rod results. With this new drive gear design a 1-degree rotation of the worm gear results in a pressure rod drive of $0.0706\mu\text{m}$, which is quite adequate for the precision repositioning of the long-path output beam.

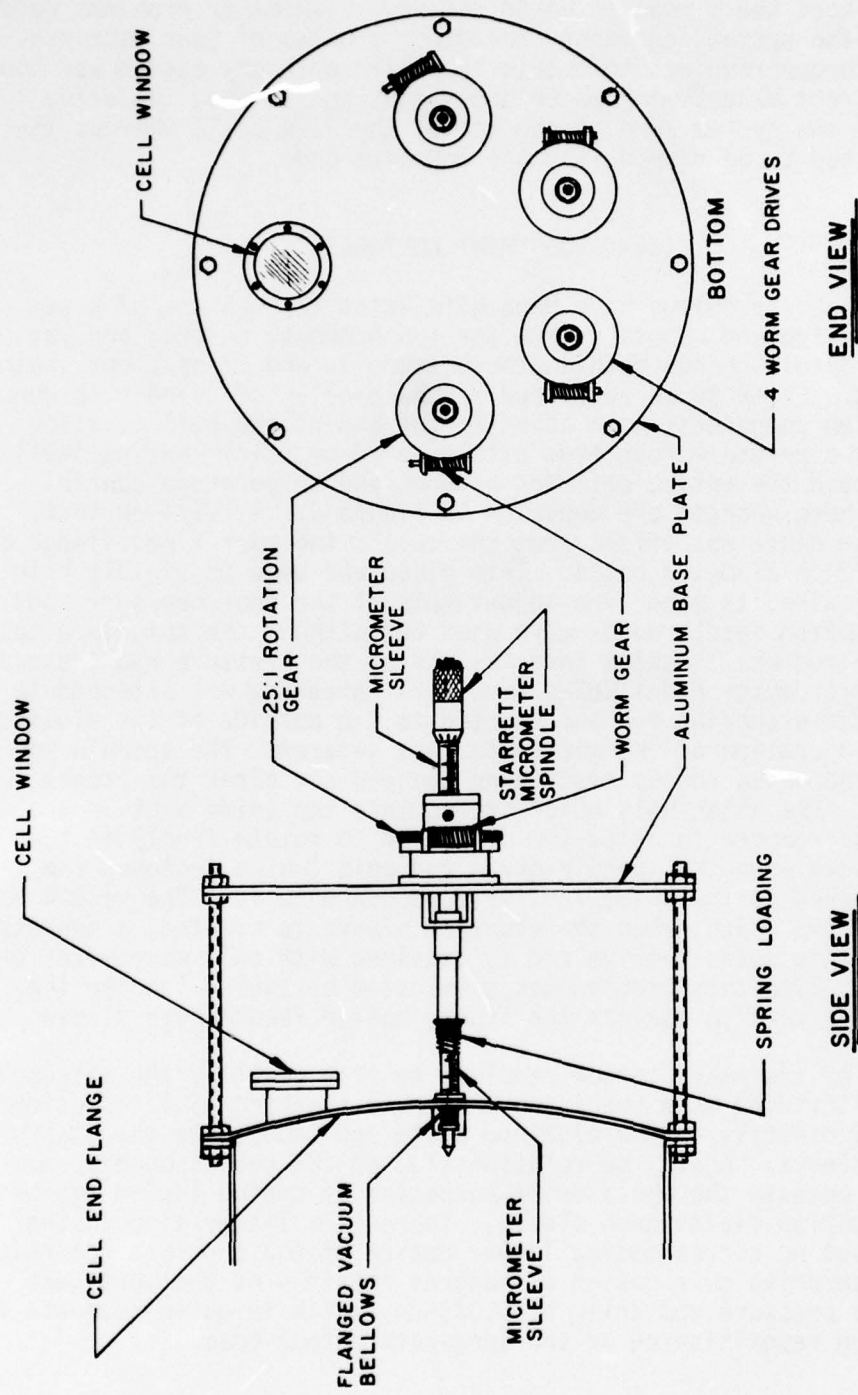


Figure 4. Aluminum base plate (end and side views) with attachment to the double-mirror end cell flange, new low-torque micrometer drive, and spring loaded attachment of the new drive to the old pressure rod and vacuum bellows arrangement.

The problem of remote control will now be addressed. Basically a selsyn transmitter and receiver are used to obtain 1:1 remote drive of the worm gear on the low-torque micrometer drive system (Figure 5). The selsyn transmitters are controlled by a 7-cm diameter dial graduated in degrees. The transmitters are located at the single-mirror end of the absorption cell where the cell output beam can be adjusted and observed simultaneously. The procedure for aligning and changing cell pathlengths will be discussed later, but the mechanical requirements for rapid remote changes between a long and short multipath will be discussed now. For changing from a 1- to a 37-spot multipath in the 21-m cell, the pressure rod must be driven 0.757 mm or 29.8 revolutions of the worm gear controlling rotation of mirror M_3 about its vertical axis. This is impractical for rapid pathlength changes. Two step-up gears are used to alleviate this system operation problem. First, a 1:4.75 step-up gear is used between the worm gear and the selsyn receiver to reduce the fine adjustment of the remote control of the linear pressure rod drive to $0.318\mu\text{m}$ per degree rotation of the selsyn transmitter dial. Obtaining the required $0.143\mu\text{m}$ linear drive precision is still routinely possible. Next a coarse adjustment dial is attached to the selsyn transmitter fine adjustment dial by a 1:5 step-up gear. As a result, only a little over one revolution of the coarse adjustment dial is required to make the 1- to 37-spot multipath change since the total gear step-up over the worm gear drive is 1:23.75. By use of this arrangement, both remote beam positioning and rapid pathlength change requirements are satisfied.

LASER ALIGNMENT

The alignment of any optical system containing light sources is greatly facilitated when the sources are of visible wavelengths. This is especially true for the precision alignment required to perform long-path absorption cell experiments. A cw helium-neon (He-Ne) laser is usually used to obtain the optical system alignment required. The light source of interest, which in the case of most EO and HEL systems is in the infrared and hence is invisible to the naked eye, is then made to propagate colinear with the He-Ne laser.

A detailed setup of an experiment using a 21-m stainless steel White cell and a line tunable pulsed deuterium fluoride (DF) laser source (Figure 6) will be used to illustrate the types of problems encountered in making long-path absorption cell measurements [9]. A Lumonics Model TEA-201 pulsed (0.3 Hz), line tunable, DF laser is used which has an unstable resonator front reflector and a grating back reflector for line selection. The resulting output is donut-shaped in the near field and has a central maximum diffraction ring pattern in the far field (25 m away) where the beam is collected by a spherically concave mirror CM_1 . The He-Ne alignment laser is made colinear with the DF laser by use of several flat mirrors M and one mirror M' with a 1-cm diameter hole drilled through the center to allow the He-Ne beam to pass through. The donut-shaped DF beam with an outside diameter of 4 cm and inside diameter of 2 cm is centered on mirror M' about the central hole by using a sheet of

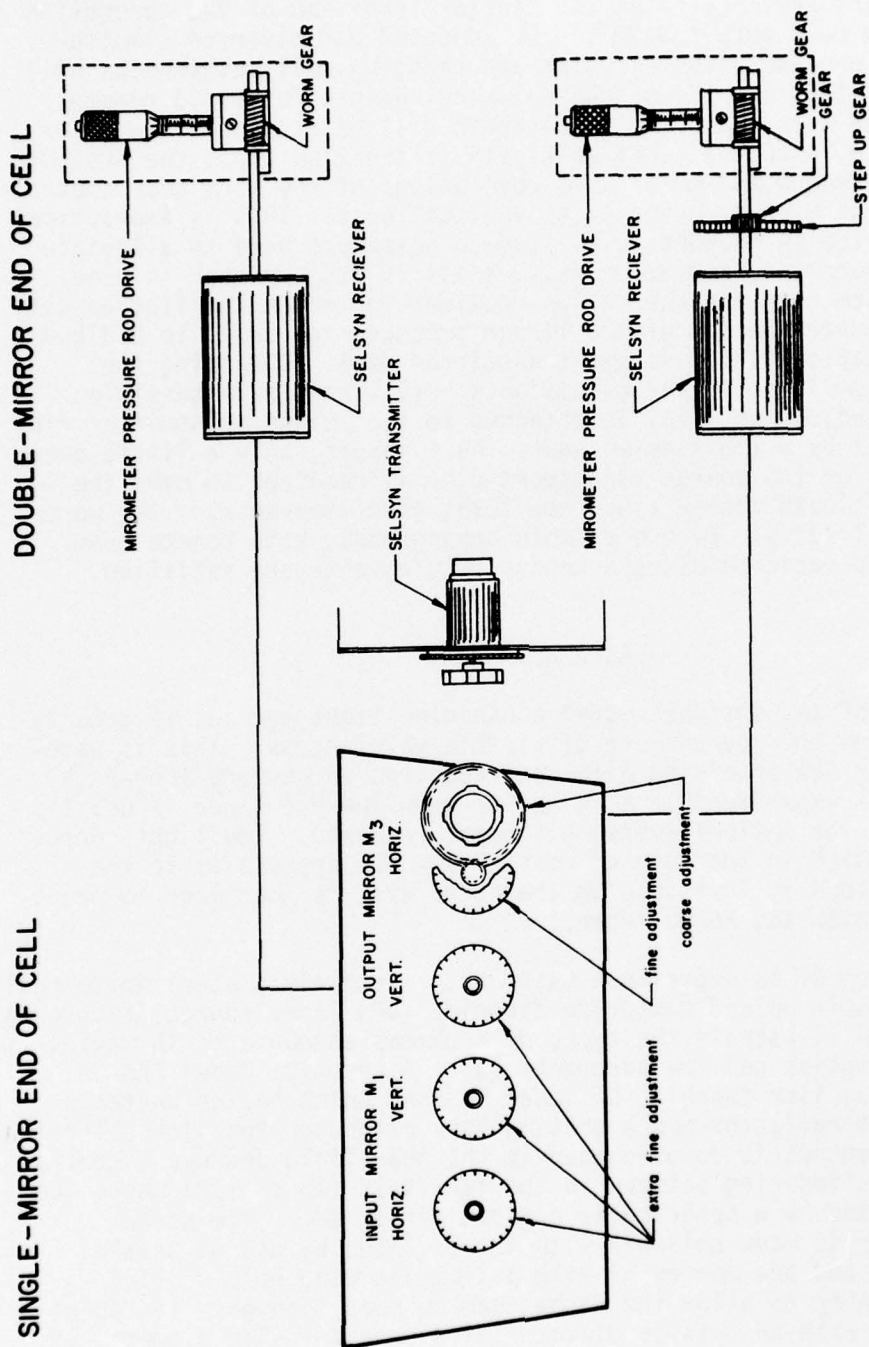


Figure 5. Remote selsyn transmitter and receiver arrangement including both the 1:1 and the stepped-up gear drives.

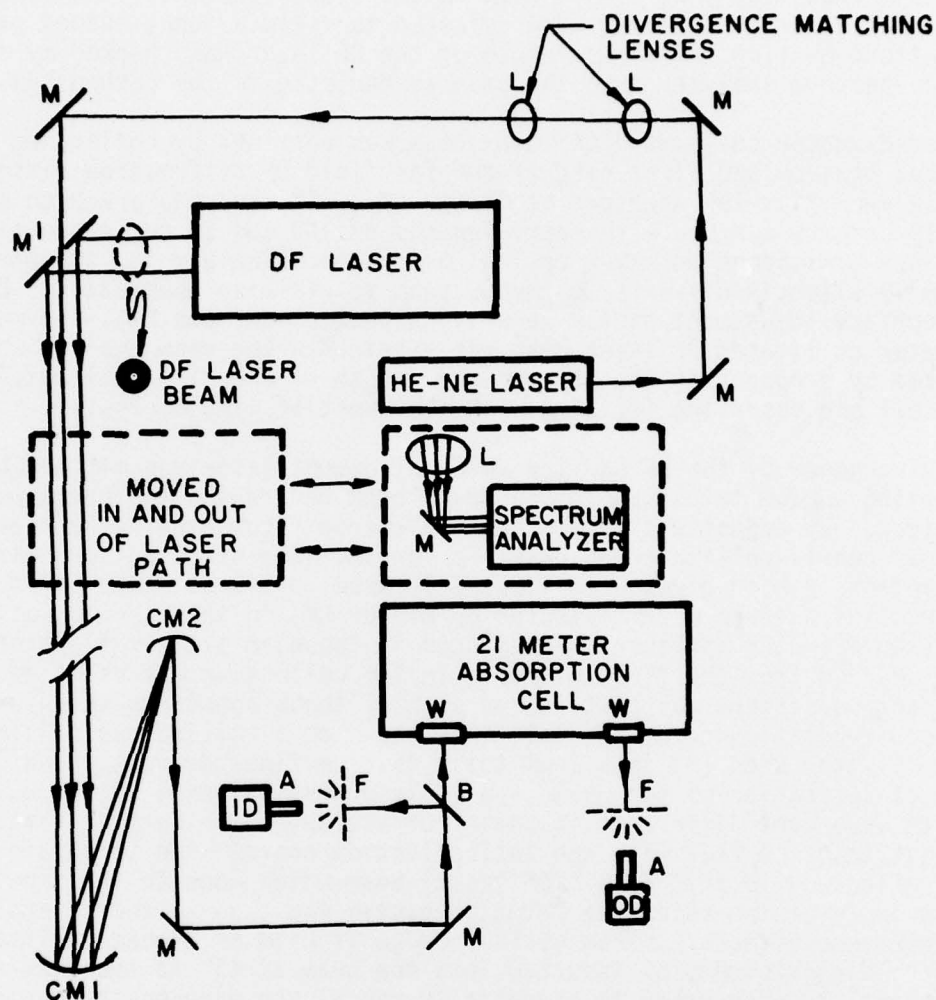


Figure 6. Experimental setup for an experiment using a DF laser source and the ASL 21-m absorption cell: He-Ne alignment laser with adjustment mirrors M; L, divergence matching and focusing lenses; M', special mirror with central hole; spectrum analyzer; CM₁ and CM₂, collection and collimating spherically concave mirrors; B, 2-mm thick calcium fluoride beam splitter; F, Teflon diffuse transmittance filters; A, detector apertures; and ID and OD, input and output indium antimonide detectors, respectively.

high sensitivity Edmund Scientific Company liquid crystal. The mode quality of the DF laser was checked by focusing the 4-cm diameter near-field beam with a calcium fluoride lens L to a few millimeters in diameter and observing the focused beam on the liquid crystal. The laser front reflector and grating were adjusted to yield a donut-shaped pattern of uniform heating. The wavelength of the DF laser was checked by inserting a spectrum analyzer into the beam as depicted in the dashed box.

A 5-mm diameter collimated DF laser beam was obtained by collecting the central maximum and first ring of the far-field DF diffraction pattern with a 4-cm diameter aperture at mirror CM₁. CM₁ and CM₂ are both spherically concave mirrors with focal lengths of 160 and 20 cm, respectively. They are positioned on a 2-m optical bench approximately 180 cm apart and only slightly off-axis to the DF beam to minimize aberration. By appropriate adjustment of the separation between CM₁ and CM₂, a 5-mm diameter collimated DF laser beam was obtained. The beam quality was checked by propagating the DF beam the length of the 21-m cell outside the cell and observing its size with the sheet of liquid crystal.

The divergence of the DF and the He-Ne alignment laser was matched by inserting a beam telescope in the He-Ne beam before the two beams were combined. By adjustment of the beam telescope focus, the He-Ne beam was made as nearly collimated as possible for the separation between mirrors CM₁ and CM₂, which gives a collimated DF beam. Several rings of an He-Ne diffraction pattern were collected by mirror CM₂ in this configuration. Two 1-cm diameter apertures were placed in the beam after reflections from CM₂ and from the first mirror M in the collection optics. The He-Ne diffraction pattern was centered on each of these apertures to ensure uniform repositioning of the cell input beam on a routine basis. The beam splitter used (B) is a 2-mm thick calcium fluoride flat which causes minimal separation of the He-Ne and DF laser optical axes due to wavelength dependent difference in their refraction by the optical flat. It is best to use a flat with one antireflection coated side to obtain only one reflected (in this case a DF laser) beam which goes to the input detector ID of the reference detector system and also to reduce etalon interference effects. If an optical wedge is used as a beam splitter, a matched pair should be inserted into the beam at 45° to the beam and orthogonal to each other to essentially cancel the wavelength dependent refraction effects. Care must be taken in selection of an appropriate beam splitter so as not to alter the colinearity of the He-Ne and DF lasers because of the exacting requirements of long-path absorption cell optical alignment.

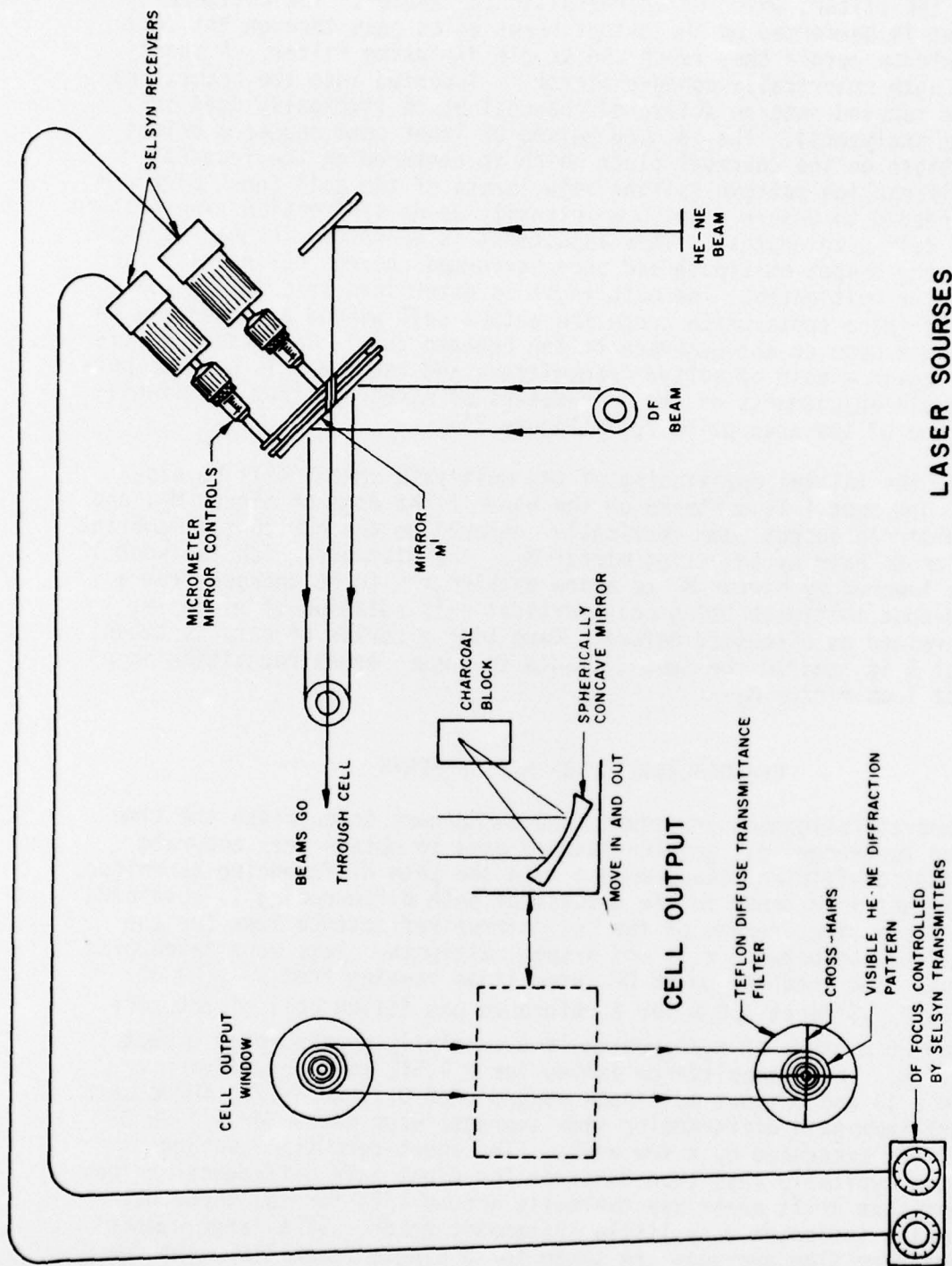
The two beams which go to the input (ID) and output (OD) detectors of the reference and sample detector systems are centered on cross hairs on specially selected diffuse transmittance filters F (diffuse reflectors could also be used). For the case of DF, Millipore LSWP04700 Teflon membrane filters have relatively flat forward lobe diffuse transmittance and work well as diffusers of DF radiation reducing the effects of beam jitter and wander. Apertures A are used to select a small enough solid angle of the diffused laser beam to ensure linear detector response.

Additionally, the He-Ne alignment beam diffraction pattern can be seen through the filter, which makes repositioning easier. The colinearity alignment is performed on the output beams which pass through the cell output window before they reach the sample diffusing filter. A short focal length spherically concave mirror is inserted into the beams, and they are focused onto an activated charcoal block (typically used in spectrum analyzers). The focused pulsed DF laser beam causes a bright burn pattern on the charcoal block which is centered on the focused He-Ne diffraction pattern (slight adjustments of the cell input mirror M may be needed to ensure a uniform intensity He-Ne diffraction ring pattern at long cell pathlengths). This adjustment is performed for each change to the long N-spot multipath and once performed ensures colinearity for all shorter multipaths. The pathlength is determined by counting the number of image spots which cross the output cell window by observing the He-Ne laser beam on the membrane filter between the 1- and N-spot multipaths. Again a pair of selsyn transmitters and receivers is used to perform remote adjustments of the micrometers of mirror M' from the single-mirror end of the absorption cell (Figure 7).

Finally, the initial positioning of the multipath spot 1 will be discussed. The spot 1 is centered on the upper right edge of mirror M₂, and its semicircle output beam vertically centered on the horizontal membrane filter cross hair by adjusting mirror M₁. The distance which the spot 1 must be lowered by mirror M₁ to allow pathlengths to be changed from a 1- to an N-spot multipath using only vertical axis rotation of mirror M₃ is determined as discussed before. Each time a series of data is taken, the spot 1 is lowered the same distance to ensure exact repositioning of the spot 1 on mirror M₂.

REPRODUCIBILITY OF MEASUREMENTS

The elaborate alignment procedures and techniques to decrease the time required to change cell pathlengths are used to obtain very accurate absorption coefficient measurements with the path differencing technique. Of paramount importance to the success of path differencing is obtaining a short-term time average of the cell mirror reflectance loss for the path difference between a 1- and N-spot multipath. Data were taken over a 2-month time interval on 26 DF laser lines ranging from P_{1_0}(2) at 3.5 μ m to P_{3_2}(11) at 4.0 μ m for a reference gas filled cell of 760 torr of an 80/20 mixture of N₂/O₂ which is essentially nonabsorbing except near 4.0 μ m. The transmittance values for a 1.512 km path difference between a 1- and 37-spot multipath ranged from 0.11 to 0.17. Three sets of short-term path differencing time averages were taken for all 26 DF laser lines separated by a few weeks. The short-term time averages exhibited typically less than 2% error for eight path differences values. The long-term drift error was typically around 1/2% for the three data sets, which indicates very little systematic error. If a large number of short-term time averages are taken for a single laser line, the long-term reflectance loss may contain less than 1/2% error. Even with the



LASER SOURCES

Figure 7. Output beam alignment scheme using He-Ne diffraction pattern, charcoal block, and remote selsyn controls of the special mirror M_1 with the centra' hole.

1/2% transmittance measurement accuracy for a 1.512 km path difference, absorptions of a few percent per kilometer have already been made [12].

CONCLUSION

Several improvements have been made in long-path absorption cell measurement capabilities which enable a single person to operate a 21-m White cell and obtain state-of-the-art measurement accuracy. Among the improvements are the low-torque linear drives for vacuum feedthrough pressure rods, remote operation for cell mirror adjustment and laser alignment using selsyn transmitters and receivers, and a variety of detection and alignment techniques. These improvements have extended the capabilities of long-path absorption cells, so that timely measurements of low absorption coefficients such as the water vapor continuum at room temperature between 3.5 and 4.0 μm are now routine. Some of the techniques discussed may also be very useful in other measurement fields.

REFERENCES

1. White, K. O., and W. R. Watkins. "Erbium Laser as Remote Sensor of Methane." Applied Optics 14 (December 1975): 2812.
2. Burch, D. E., E. B. Singleton, and D. Williams. "Absorption Line Broadening in the Near Infrared." Applied Optics 1 (1962): 359.
3. Burch, D. E., D. A. Gryvnak, and J. D. Pembroke. "Investigation of the Absorption of Infrared Radiation by Atmospheric Gases: Water, Nitrogen, Nitrous Oxide." AFCRL-71-0124, Air Force Cambridge Research Laboratories, Hanscom Air Force Base, Maine, January 1971, 32 pp.
4. Bruce, C. W., B. Z. Sojka, B. G. Hurd, W. R. Watkins, K. O. White, and Z. Derzko. "Application of Pulsed-Source Spectrophone to Absorption by Methane at DF Laser Wavelengths." Applied Optics 15 (December 1976): 2970.
5. White, K. O., G. T. Wade, and S. A. Schleusener. "The Application of Minicomputers in Laser Atmospheric Experiments." Proceedings of the Institute of Electrical and Electronics Engineers 61 (November 1973): 1596.
6. Watkins, W. R. "Improvements in Long Path Absorption Cell Measurements." ECOM-5586, Atmospheric Sciences Laboratory, US Army Electronics Command, White Sands Missile Range, New Mexico, March 1976, 35 pp.
7. Watkins, W. R. "Path Differencing: An Improvement to Multipass Absorption Cell Measurements." Applied Optics 15 (January 1976): 16.
8. White, K. O., W. R. Watkins, S. A. Schleusener, and R. L. Johnson. "Multiwavelength Discriminator and Display System for Solid-State Lasers." Review of Scientific Instruments 47 (June 1976): 695.
9. White, K. O., and W. R. Watkins. "Absorption of DF Laser Radiation by Propane and Butane." ECOM-5563, Atmospheric Sciences Laboratory, US Army Electronics Command, White Sands Missile Range, New Mexico, June 1975, 15 pp.
10. White, J. U. "Long Optical Paths of Large Aperture." Journal of the Optical Society of America 32 (May 1942): 285.
11. White, J. U. "Very Long Optical Paths in Air." Journal of the Optical Society of America 66, (May 1976): 411.
12. White, K. O., W. R. Watkins, and C. W. Bruce. "Absorption of Atmospheric Gases in the Deuterium Fluoride Spectral Region: 3.5 - 4.0 μ m." Great Lakes Training Center, Illinois, Proceedings of the Twenty-Fourth National Infrared Information Symposium, August 1976 (in press).

DISTRIBUTION LIST

Director
US Army Ballistic Research Laboratory
ATTN: DRDAR-BLB, Dr. G. E. Keller
Aberdeen Proving Ground, MD 21005

Air Force Weapons Laboratory
ATTN: Technical Library (SUL)
Kirtland AFB, NM 87117

Commander
Headquarters, Fort Huachuca
ATTN: Tech Ref Div
Fort Huachuca, AZ 85613

6585 TG/WE
Holloman AFB, NM 88330

Commandant
US Army Field Artillery School
ATTN: Morris Swett Tech Library
Fort Sill, OK 73503

Commandant
USAFAS
ATTN: ATSF-CD-MT (Mr. Farmer)
Fort Sill, OK 73503

Director
US Army Engr Waterways Exper Sta
ATTN: Library Branch
Vicksburg, MS 39180

Commander
US Army Electronics Command
ATTN: DRSEL-CT-S (Dr. Swingle)
Fort Monmouth, NJ 07703
03

CPT Hugh Albers, Exec Sec
Interdept Committee on Atmos Sci
Fed Council for Sci & Tech
National Sci Foundation
Washington, DC 20550

Inge Dirmhirn, Professor
Utah State University, UMC 48
Logan, UT 84322

HQDA (DAEN-RDM/Dr. De Percin)
Forrestal Bldg
Washington, DC 20314

Commander
US Army Aviation Center
ATTN: ATZQ-D-MA
Fort Rucker, AL 36362

CO, USA Foreign Sci & Tech Center
ATTN: DRXST-ISI
220 7th Street, NE
Charlottesville, VA 22901

Director
USAE Waterways Experiment Station
ATTN: Library
PO Box 631
Vicksburg, MS 39180

US Army Research Office
ATTN: DRXRO-IP
PO Box 12211
Research Triangle Park, NC 27709

Mr. William A. Main
USDA Forest Service
1407 S. Harrison Road
East Lansing, MI 48823

Library-R-51-Tech Reports
Environmental Research Labs
NOAA
Boulder, CO 80302

Commander
US Army Dugway Proving Ground
ATTN: MT-S
Dugway, UT 84022

HQ, ESD/DRI/S-22
Hanscom AFB
MA 01731

Head, Atmospheric Rsch Section
National Science Foundation
1800 G. Street, NW
Washington, DC 20550

Office, Asst Sec Army (R&D)
ATTN: Dep for Science & Tech
HQ, Department of the Army
Washington, DC 20310

Commander
US Army Satellite Comm Agc
ATTN: DRCPM-SC-3
Fort Monmouth, NJ 07703

Sylvania Elec Sys Western Div
ATTN: Technical Reports Library
PO Box 205
Mountain View, CA 94040

William Peterson
Research Association
Utah State University, UNC 48
Logan, UT 84322

Defense Communications Agency
Technical Library Center
Code 205
Washington, DC 20305

Dr. A. D. Belmont
Research Division
PO Box 1249
Control Data Corp
Minneapolis, MN 55440

Commander
US Army Electronics Command
ATTN: DRSEL-WL-D1
Fort Monmouth, NJ 07703

Commander
ATTN: DRSEL-VL-D
Fort Monmouth, NJ 07703

Meteorologist in Charge
Kwajalein Missile Range
PO Box 67
APO
San Francisco, CA 96555

The Library of Congress
ATTN: Exchange & Gift Div
Washington, DC 20540
2

US Army Liaison Office
MIT-Lincoln Lab, Library A-082
PO Box 73
Lexington, MA 02173

Dir National Security Agency
ATTN: TDL (C513)
Fort George G. Meade, MD 20755

Director, Systems R&D Service
Federal Aviation Administration
ATTN: ARD-54
2100 Second Street, SW
Washington, DC 20590

Commander
US Army Missile Command
ATTN: DRSMI-RRA, Bldg 7770
Redstone Arsenal, AL 35809

Dir of Dev & Engr
Defense Systems Div
ATTN: SAREA-DE-DDR
H. Tannenbaum
Edgewood Arsenal, APG, MD 21010

Naval Surface Weapons Center
Technical Library & Information
Services Division
White Oak, Silver Spring, MD
20910

Dr. Frank D. Eaton
PO Box 3038
Universtiy Station
Laramie, Wyoming 82071

Rome Air Development Center
ATTN: Documents Library
TILD (Bette Smith)
Griffiss Air Force Base, NY 13441

National Weather Service
National Meteorological Center
World Weather Bldg - 5200 Auth Rd
ATTN: Mr. Quiroz
Washington, DC 20233

USAFETAC/CB (Stop 825)
Scott AFB
IL 62225

Director
Defense Nuclear Agency
ATTN: Tech Library
Washington, DC 20305

Director
Development Center MCDEC
ATTN: Firepower Division
Quantico, VA 22134

Environmental Protection Agency
Meteorology Laboratory
Research Triangle Park, NC
27711

Commander
US Army Electronics Command
ATTN: DRSEL-GG-TD
Fort Monmouth, NJ 07703

Commander
US Army Ballistic Rsch Labs
ATTN: DRXBR-IB
APG, MD 21005

Dir, US Naval Research Lab
Code 5530
Washington, DC 20375

Mil Assistant for
Environmental Sciences
DAD (E & LS), 3D129
The Pentagon
Washington, DC 20301

The Environmental Rsch
Institute of MI
ATTN: IRIA Library
PO Box 618
Ann Arbor, MI 48107

Armament Dev & Test Center
ADTC (DLOSL)
Eglin AFB, Florida 32542

Range Commanders Council
ATTN: Mr. Hixon
PMTIC Code 3252
Pacific Missile Test Center
Point Mugu, CA 93042

Commander
Eustis Directorate
US Army Air Mobility R&D Lab
ATTN: Technical Library
Fort Eustis, VA 23604

Commander
Frankford Arsenal
ATTN: SARFA-FCD-0, Bldg 201-2
Bridge & Tarcony Sts
Philadelphia, PA 19137

Director, Naval Oceanography and
Meteorology
National Space Technology Laboratories
Bay St Louis, MS 39529

Commander
US Army Electronics Command
ATTN: DRSEL-CT-S
Fort Monmouth, NJ 07703

Commander
USA Cold Regions Test Center
ATTN: STECR-OP-PM
APO Seattle 98733

Redstone Scientific Information Center
ATTN: DRDMI-TBD
US Army Missile Res & Dev Command
Redstone Arsenal, AL 35809

Commander
AFWL/WE
Kirtland AFB, NM 87117

Naval Surface Weapons Center
Code DT-22 (Ms. Greeley)
Dahlgren, VA 22448

Commander
Naval Ocean Systems Center
ATTN: Research Library
San Diego, CA 92152

Commander
US Army INSCOM
ATTN: IARDA-OS
Arlington Hall Station
Arlington, VA 22212

Commandant
US Army Field Artillery School
ATTN: ATSF-CF-R
Fort Sill, OK 73503

Commander and Director
US Army Engineer Topographic Labs
ETL-GS-AC
Fort Belvoir, VA 22060

Technical Processes Br-D823
NOAA, Lib & Info Serv Div
6009 Executive Blvd
Rockville, MD 20852

Commander
US Army Missile Research
and Development Command
ATTN: DRDMI-CGA, B. W. Fowler
Redstone Arsenal, AL 35809

Commanding Officer
US Army Armament Rsch & Dev Com
ATTN: DRDAR-TSS #59
Dover, NJ 07801

Air Force Cambridge Rsch Labs
ATTN: LCB (A. S. Carten, Jr.)
Hanscom AFB
Bedford, MA 01731

National Center for Atmos Res
NCAR Library
PO Box 3000
Boulder, CO 80307

Air Force Geophysics Laboratory
ATTN: LYD
Hanscom AFB
Bedford, MA 01731

Chief, Atmospheric Sciences Division
Code ES-81
NASA
Marshall Space Flight Center, AL 35812

Department of the Air Force
OL-C, 5WW
Fort Monroe, VA 23651

Commander
US Army Missile Rsch & Dev Com
ATTN: DRDMI-TR
Redstone Arsenal, AL 35809

Meteorology Laboratory
AFGL/LY
Hanscom AFB, MA 01731

Director CFD
US Army Field Artillery School
ATTN: Met Division
Fort Sill, OK 73503

Naval Weapons Center (Code 3173)
ATTN: Dr. A. Shlanta
China Lake, CA 93555

Director
Atmospheric Physics & Chem Lab
Code R31, NOAA
Department of Commerce
Boulder, CO 80302

Department of the Air Force
5 WW/DN
Langley AFB, VA 23665

Commander
US Army Intelligence Center and School
ATTN: ATSI-CD-MD
Fort Huachuca, AZ 85613

Dr. John L. Walsh
Code 4109
Navy Research Lab
Washington, DC 20375

Director
US Army Armament Rsch & Dev Com
Chemical Systems Laboratory
ATTN: DRDAR-CLJ-I
Aberdeen Proving Ground, MD 21010

R. B. Girardo
Bureau of Reclamation
E&R Center, Code 1220
Denver Federal Center, Bldg 67
Denver, CO 80225

Commander
US Army Missile Command
ATTN: DRDMI-TEM
Redstone Arsenal, AL 35809

Commander
US Army Tropic Test Center
ATTN: STETC-MO (Tech Library)
APO New York 09827

Commanding Officer
Naval Research Laboratory
Code 2627
Washington, DC 20375

Defense Documentation Center
ATTN: DDC-TCA
Cameron Station (Bldg 5)
Alexandria, Virginia 22314
12

Commander
US Army Test and Evaluation Command
ATTN: Technical Library
White Sands Missile Range, NM 88002

US Army Nuclear Agency
ATTN: MONA-WE
Fort Belvoir, VA 22060

Commander
US Army Proving Ground
ATTN: Technical Library
Bldg 2100
Yuma, AZ 85364

Office, Asst Sec Army (R&D)
ATTN: Dep for Science & Tech
HQ, Department of the Army
Washington, DC 20310

ATMOSPHERIC SCIENCES RESEARCH PAPERS

1. Lindberg, J.D., "An Improvement to a Method for Measuring the Absorption Coefficient of Atmospheric Dust and other Strongly Absorbing Powders," ECOM-5565, July 1975.
2. Avara, Elton P., "Mesoscale Wind Shears Derived from Thermal Winds," ECOM-5566, July 1975.
3. Gomez, Richard B., and Joseph H. Pierluissi, "Incomplete Gamma Function Approximation for King's Strong-Line Transmittance Model," ECOM-5567, July 1975.
4. Blanco, A.J., and B.F. Engebos, "Ballistic Wind Weighting Functions for Tank Projectiles," ECOM-5568, August 1975.
5. Taylor, Fredrick J., Jack Smith, and Thomas H. Pries, "Crosswind Measurements through Pattern Recognition Techniques," ECOM-5569, July 1975.
6. Walters, D.L., "Crosswind Weighting Functions for Direct-Fire Projectiles," ECOM-5570, August 1975.
7. Duncan, Louis D., "An Improved Algorithm for the Iterated Minimal Information Solution for Remote Sounding of Temperature," ECOM-5571, August 1975.
8. Robbiani, Raymond L., "Tactical Field Demonstration of Mobile Weather Radar Set AN/TPS-41 at Fort Rucker, Alabama," ECOM-5572, August 1975.
9. Miers, B., G. Blackman, D. Langer, and N. Lorimier, "Analysis of SMS/GOES Film Data," ECOM-5573, September 1975.
10. Manquero, Carlos, Louis Duncan, and Rufus Bruce, "An Indication from Satellite Measurements of Atmospheric CO₂ Variability," ECOM-5574, September 1975.
11. Petracca, Carmine, and James D. Lindberg, "Installation and Operation of an Atmospheric Particulate Collector," ECOM-5575, September 1975.
12. Avara, Elton P., and George Alexander, "Empirical Investigation of Three Iterative Methods for Inverting the Radiative Transfer Equation," ECOM-5576, October 1975.
13. Alexander, George D., "A Digital Data Acquisition Interface for the SMS Direct Readout Ground Station — Concept and Preliminary Design," ECOM-5577, October 1975.
14. Cantor, Israel, "Enhancement of Point Source Thermal Radiation Under Clouds in a Nonattenuating Medium," ECOM-5578, October 1975.
15. Norton, Colburn, and Glenn Hoidale, "The Diurnal Variation of Mixing Height by Month over White Sands Missile Range, N.M.," ECOM-5579, November 1975.
16. Avara, Elton P., "On the Spectrum Analysis of Binary Data," ECOM-5580, November 1975.
17. Taylor, Fredrick J., Thomas H. Pries, and Chao-Huan Huang, "Optimal Wind Velocity Estimation," ECOM-5581, December 1975.
18. Avara, Elton P., "Some Effects of Autocorrelated and Cross-Correlated Noise on the Analysis of Variance," ECOM-5582, December 1975.
19. Gillespie, Patti S., R.L. Armstrong, and Kenneth O. White, "The Spectral Characteristics and Atmospheric CO₂ Absorption of the Ho⁺³ YLF Laser at 2.05 μ m," ECOM-5583, December 1975.
20. Novlan, David J., "An Empirical Method of Forecasting Thunderstorms for the White Sands Missile Range," ECOM-5584, February 1976.
21. Avara, Elton P., "Randomization Effects in Hypothesis Testing with Autocorrelated Noise," ECOM-5585, February 1976.
22. Watkins, Wendell R., "Improvements in Long Path Absorption Cell Measurement," ECOM-5586, March 1976.
23. Thomas, Joe, George D. Alexander, and Marvin Dubbin, "SATTEL — An Army Dedicated Meteorological Telemetry System," ECOM-5587, March 1976.
24. Kennedy, Bruce W., and Delbert Bynum, "Army User Test Program for the RDT&E-XM-75 Meteorological Rocket," ECOM-5588, April 1976.

25. Barnett, Kenneth M., "A Description of the Artillery Meteorological Comparisons at White Sands Missile Range, October 1974 - December 1974 ('PASS' - Prototype Artillery [Meteorological] Subsystem)," ECOM-5589, April 1976.
26. Miller, Walter B., "Preliminary Analysis of Fall-of-Shot From Project 'PASS'," ECOM-5590, April 1976.
27. Avara, Elton P., "Error Analysis of Minimum Information and Smith's Direct Methods for Inverting the Radiative Transfer Equation," ECOM-5591, April 1976.
28. Yee, Young P., James D. Horn, and George Alexander, "Synoptic Thermal Wind Calculations from Radiosonde Observations Over the Southwestern United States," ECOM-5592, May 1976.
29. Duncan, Louis D., and Mary Ann Seagraves, "Applications of Empirical Corrections to NOAA-4 VTPR Observations," ECOM-5593, May 1976.
30. Miers, Bruce T., and Steve Weaver, "Applications of Meteorological Satellite Data to Weather Sensitive Army Operations," ECOM-5594, May 1976.
31. Sharenow, Moses, "Redesign and Improvement of Balloon ML-566," ECOM-5595, June, 1976.
32. Hansen, Frank V., "The Depth of the Surface Boundary Layer," ECOM-5596, June 1976.
33. Pinnick, R.G., and E.B. Stenmark, "Response Calculations for a Commercial Light-Scattering Aerosol Counter," ECOM-5597, July 1976.
34. Mason, J., and G.B. Hoidale, "Visibility as an Estimator of Infrared Transmittance," ECOM-5598, July 1976.
35. Bruce, Rufus E., Louis D. Duncan, and Joseph H. Pierluissi, "Experimental Study of the Relationship Between Radiosonde Temperatures and Radiometric-Area Temperatures," ECOM-5599, August 1976.
36. Duncan, Louis D., "Stratospheric Wind Shear Computed from Satellite Thermal Sounder Measurements," ECOM-5800, September 1976.
37. Taylor, F., P. Mohan, P. Joseph and T. Pries, "An All Digital Automated Wind Measurement System," ECOM-5801, September 1976.
38. Bruce, Charles, "Development of Spectrophones for CW and Pulsed Radiation Sources," ECOM-5802, September 1976.
39. Duncan, Louis D., and Mary Ann Seagraves, "Another Method for Estimating Clear Column Radiances," ECOM-5803, October 1976.
40. Blanco, Abel J., and Larry E. Taylor, "Artillery Meteorological Analysis of Project Pass," ECOM-5804, October 1976.
41. Miller, Walter, and Bernard Engebos, "A Mathematical Structure for Refinement of Sound Ranging Estimates," ECOM-5805, November, 1976.
42. Gillespie, James B., and James D. Lindberg, "A Method to Obtain Diffuse Reflectance Measurements from 1.0 to 3.0 μ m Using a Cary 17I Spectrophotometer," ECOM-5806, November 1976.
43. Rubio, Roberto, and Robert O. Olsen, "A Study of the Effects of Temperature Variations on Radio Wave Absorption," ECOM-5807, November 1976.
44. Ballard, Harold N., "Temperature Measurements in the Stratosphere from Balloon-Borne Instrument Platforms, 1968-1975," ECOM-5808, December 1976.
45. Monahan, H.H., "An Approach to the Short-Range Prediction of Early Morning Radiation Fog," ECOM-5809, January 1977.
46. Engebos, Bernard Francis, "Introduction to Multiple State Multiple Action Decision Theory and Its Relation to Mixing Structures," ECOM-5810, January 1977.
47. Low, Richard D.H., "Effects of Cloud Particles on Remote Sensing from Space in the 10-Micrometer Infrared Region," ECOM-5811, January 1977.
48. Bonner, Robert S., and R. Newton, "Application of the AN/GVS-5 Laser Rangefinder to Cloud Base Height Measurements," ECOM-5812, February 1977.

49. Rubio, Roberto, "Lidar Detection of Subvisible Reentry Vehicle Erosive Atmospheric Material," ECOM-5813, March 1977.
50. Low, Richard D.H., and J.D. Horn, "Mesoscale Determination of Cloud-Top Height: Problems and Solutions," ECOM-5814, March 1977.
51. Duncan, Louis D., and Mary Ann Seagraves, "Evaluation of the NOAA-4 VTPR Thermal Winds for Nuclear Fallout Predictions," ECOM-5815, March 1977.
52. Randhawa, Jagir S., M. Izquierdo, Carlos McDonald and Zvi Salpeter, "Stratospheric Ozone Density as Measured by a Chemiluminescent Sensor During the Stratcom VI-A Flight," ECOM-5816, April 1977.
53. Rubio, Roberto, and Mike Izquierdo, "Measurements of Net Atmospheric Irradiance in the 0.7- to 2.8-Micrometer Infrared Region," ECOM-5817, May 1977.
54. Ballard, Harold N., Jose M. Serna, and Frank P. Hudson Consultant for Chemical Kinetics, "Calculation of Selected Atmospheric Composition Parameters for the Mid-Latitude, September Stratosphere," ECOM-5818, May 1977.
55. Mitchell, J.D., R.S. Sagar, and R.O. Olsen, "Positive Ions in the Middle Atmosphere During Sunrise Conditions," ECOM-5819, May 1977.
56. White, Kenneth O., Wendell R. Watkins, Stuart A. Schleusener, and Ronald L. Johnson, "Solid-State Laser Wavelength Identification Using a Reference Absorber," ECOM-5820, June 1977.
57. Watkins, Wendell R., and Richard G. Dixon, "Automation of Long-Path Absorption Cell Measurements," ECOM-5821, June 1977.